

Modeling and Analysis of the Toyota Hybrid System

Jinming Liu, Huei Peng and Zoran Filipi

Abstract—Toyota Hybrid System is the innovative powertrain used in the current best-selling hybrid vehicle on the market—the Prius. It uses a split-type hybrid configuration which contains both a parallel and a serial power path to achieve the benefits of both. The main purpose of this paper is to develop a dynamic model to investigate the unique design of THS, which will be used to analyze the control strategy, and explore the potential of further improvement. A Simulink model is developed and a control algorithm is derived. Simulations confirm our model captures the fundamental behavior of THS reasonably well.

I. INTRODUCTION

DUE to their significant potential in reducing fuel consumption and emissions, hybrid electric vehicles (HEV) are now actively developed by many car companies. In the late 1997, Toyota Motor Corp. released the first generation Prius, which features the Toyota hybrid system (THS). The MY2004 Prius model is based on an improved power train, the THS-II, with significantly improved vehicle performance, interior volume, and fuel economy. The new Prius is quite popular and has reached a sales volume of about 5,500 car/month. A scaled-up and more sophisticated version of THS (a.k.a. Toyota Synergy Drive) is being developed and two hybrid SUVs (Highlander and Lexus RX 400H) will be offered by Toyota within MY2005.

The power train configuration of THS is intriguing because it does not belong to the conventional categories of either series or parallel hybrids. For these two simpler hybrid configurations, the operation of the power train is relatively easy to understand. For example, Honda's hybrid Civic with the integrated motor assist system (IMA) [1] clearly belongs to the parallel type, albeit it is a "mild" hybrid. Many prototype hybrid buses and trucks use the series hybrid configuration because of the simpler power transfer layout and control strategy. Duoba et al. [2] provided in-depth characterization and experimental comparison of two of the earliest production hybrid vehicles—Toyota Prius and Honda Insight. Both vehicles offer lower emissions and much improved fuel economy compared with their conventional counterparts.

Both parallel and series configurations have been widely studied and there has been a wealth of literature [3-7]. The parallel configuration, as shown in Fig. 1 A, includes two

separate power paths. When the secondary power source is small ("Mild" hybrids), the control problem becomes much simpler, as the two power sources do not work simultaneously. When the motor is relative large ("Full" hybrids), the internal combustion engine and electrical motor can drive the vehicle individually or simultaneously. The basic role of the motor is to help the engine to operate efficiently and to capture regenerative braking energy. However, the control algorithm can be a lot more elaborate [4]. The series configuration, as shown in Fig. 1 B, only has the motor (sometime motors) driving the wheels—the engine is not directly connected to the wheels. The motor power is supplied by either battery or the generator. Since the engine operation is independent from the vehicle speed and road condition, it can operate near the optimal condition most of the time. In addition, the loss due to torque converter and transmission is avoided.

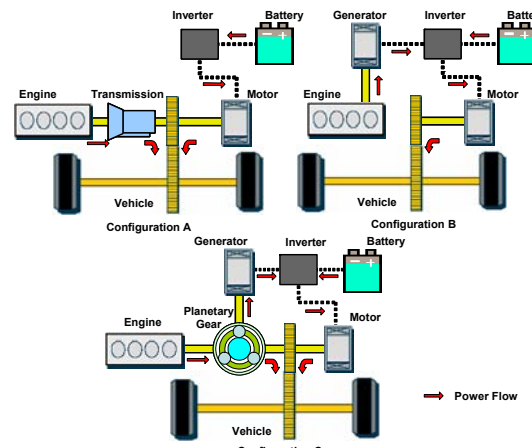


Fig. 1. Hybrid vehicle configurations: A. Parallel; B. Series; C. Power Split (parallel/series).

The THS uses a planetary gear set to connect the three power sources including an engine, a motor, and a generator. Since both the motor and the generator can operate in both charging and discharging modes, they are sometimes denoted as Motor/Generator 1 and Motor/Generator 2. We will use the former naming scheme to reflect their major roles. As shown in Fig. 1 C, it has both a parallel power path and a series power path. In addition, the planetary gear set provides infinite gear ratio between the engine and the vehicle speed so it is both a power summing device and a gear ratio device. Because of the complexity of the system, more elaborate control algorithm needs to be designed. A split-type hybrid vehicle model was developed and optimal control algorithm studied in [8] by using the dynamic programming technique. Their

Manuscript received March 1, 2005.

The authors are all with the Department of Mechanical Engineering, University of Michigan, Ann Arbor, MI, 48109-2133 USA. (contact: hpeng@umich.edu).

dynamic model does not analyze detail component behavior. A MY2000 Toyota Prius vehicle (which was sold only in Japan) was analyzed in [9][10]. They developed vehicle models in PSAT and ADVISOR ([11][12]). Rizoulis et al. [13] presented a mathematical model of a vehicle with a power split device based on the steady state transmission performance. Despite of these early efforts, to our knowledge a complete forward-looking dynamic model including the hybrid control algorithm does not yet exist in the literature.

Based on the information on THS and the new THS-II (Muta, at al. [14]), we found that the enhancement from the first generation to second generation of THS includes improved component sizing, higher efficiency, and increased generator operating range. It appears that the power split gear set remains the same—i.e., the basic dynamic equations governing the vehicle remain unchanged. Due to the fact much more information was available about THS (e.g., [2], [9]-[12]), compared with THS-II ([14]), we decided to develop a dynamic model based on THS (and the MY2000 Prius). We believe such a model is still valuable. When detailed information about THS-II become available, a model can be easily constructed based on the same model architecture.

In summary, the main contribution of this paper is the development and analysis of a dynamic model of the THS system. Due to the fact that the planetary gear plays the central role of integrating the power devices together, we will focus around the planetary gear and derive associated dynamic equations.

II. DYNAMIC MODEL

Fig. 2 shows the power train configuration of the THS. The planetary gear has three nodes: the sun gear, the carrier gear, and the ring gear; which are connected to the generator, engine and vehicle, respectively. In addition, an electric motor is also attached to the ring gear, which enables direct motor propulsion and efficient regenerative braking. The power generated by the engine is transferred to the vehicle through two paths: a mechanical path and an electrical path. The mechanical path consists of power transfer from the carrier gear directly to the ring gear, which is connected to the final drive of the vehicle. Part of the engine power transfers through the sun gear. The power is then transformed to the electrical form through the generator. The power is then either pumped into the battery, or to the electric motor. Obviously, engine power going through the second (electrical) path is less efficient than the mechanical path from an instantaneous viewpoint. However, the energy stored in the battery may be used later in a more efficient manner which helps to improve the overall vehicle fuel economy.

A. Planetary Gear

As a result of the mechanical connection through gear

teeth meshing, the rotational speed of the ring gear ω_r , sun gear ω_s , and the carrier gear ω_c satisfy the following relationship at all times:

$$\omega_s S + \omega_r R = \omega_c (R + S) \quad (1)$$

where R , and S are the radii (or number of teeth) of the ring gear and sun gear respectively.

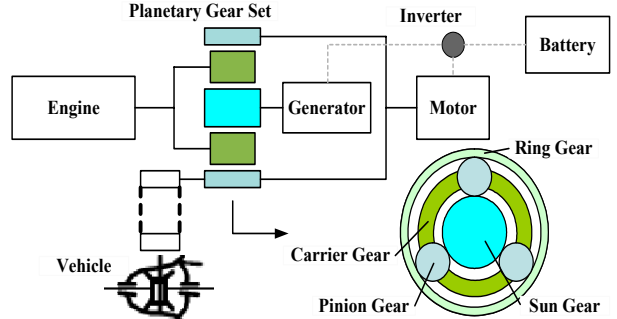


Fig. 2. Power train configuration of the Toyota Hybrid System.

Because of the speed constraint shown in equation (1), the planetary gear, despite of the fact it has three “nodes”, only has two degrees of freedom. But since there are three power devices connected to the planetary gear, three input torques, from engine, motor, and generator can all be specified independently. The rotational speeds are then calculated based on the Euler equation.

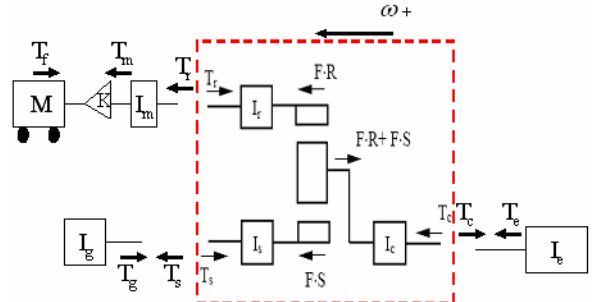


Fig. 3. Free body diagram of the mechanical path.

The free body diagram, with the rotational degrees of freedom shown in (conceptually) translational motions, is illustrated in Fig. 3. The planetary gear system is highlighted in the dash-line box, which shows the internal forces between the gears. The mass of the pinion gears is assumed to be small and the pinion gears simply serve as an ideal force transfer mechanism. By applying the Euler's law, we have

$$\dot{\omega}_r I_r = F \cdot R - T_r \quad (2)$$

$$\dot{\omega}_c I_c = T_c - F \cdot R - F \cdot S \quad (3)$$

$$\dot{\omega}_s I_s = F \cdot S - T_s \quad (4)$$

where T_r , T_s , and T_c are the torques on the ring gear shaft, the sun gear shaft, and the carrier shaft respectively, I_r , I_s , and I_c are the corresponding inertia. F presents the internal force on the pinion gear. To simplify the equations, we assume there is no viscous or Coulomb friction.

Outside of the planetary gear, the three power sources each exert a torque to their respective inertia to affect the

motion of the overall system. It can be seen that for all the inertias, moving to the left denotes positive motion, and positive engine torque and motor torque both results in vehicle acceleration. The generator torque, on the other hand, was defined to be positive to resist the vehicle motion. In other words, a positive generator torque intends to slow down the vehicle motion and extract power from the system. For the generator inertia, the governing equation is:

$$\dot{\omega}_g I_g = T_s - T_g \quad (5)$$

where T_g is the input torque from the generator, ω_g and I_g , are its rotary speed and inertia. From (4) and (5), we have,

$$\dot{\omega}_g (I_g + I_s) = F \cdot S - T_g \quad (6)$$

Similarly, on the carrier gear shaft, the engine speed is governed by the equation

$$\dot{\omega}_e I_e = T_e - T_c \quad (7)$$

where T_e is the engine torque, ω_e and I_e , are the engine rotational speed and inertia. From (3) and (7)

$$\dot{\omega}_e (I_e + I_c) = T_e - F \cdot R - F \cdot S \quad (8)$$

The dynamic equation for the ring gear is more complicated because both of the load torque, motor torque, and final drive. Here we only consider the vehicle longitudinal dynamics, and we assume there is no tire slip or efficiency loss in the driveline. This will simplify the system equation but might result in slightly higher fuel economy prediction. The governing equation for the ring gear assembly all the way through the vehicle, assuming perfect mechanical linkage, becomes

$$\begin{aligned} \dot{\omega}_r \left(\frac{R^2}{K} m + I_m K \right) &= (T_r + T_m) K - T_{fb} - mgf_r R_{tire} \\ &\quad - 0.5\rho A C_d \left(\frac{\omega_r}{K} \right)^2 R_{tire} \end{aligned} \quad (9)$$

where T_m is the motor torque, T_{fb} is the brake torque applied by the traditional friction brake system. K is the final drive ratio, R_{tire} is the tire radius, f_r is the rolling resistance coefficient, and $0.5\rho A C_d$ presents the aerial dynamic drag resistance. I_m is the inertia of the motor. From (2) and (9)

$$\begin{aligned} \dot{\omega}_r \left(\frac{R^2}{K} m + I_m K + I_r K \right) &= (T_m + F \cdot R) K - T_{fb} \\ &\quad - mgf_r R_{tire} - 0.5\rho A C_d \left(\frac{\omega_r}{K} \right)^2 R_{tire}^3 \end{aligned} \quad (10)$$

Equations (6), (8), and (10) now represent the relations between the rotational motions of the generator, engine, and vehicle. Note that the motor is directly attached to the drive axle so motor speed is not a separate degree of freedom. There are four unknown variables: three speeds and the internal force on the pinion gear (i.e. force F). Apply Eq.(1) and eliminate the internal force from the equations, we obtain

$$\begin{aligned} \left(\frac{I_v}{R I_e K} + \frac{S^2 I_v}{R I_g K} + R \right) \dot{\omega}_r &= \left(\frac{(R+S)^2}{R I_e} + \frac{S^2}{R I_g} \right) T_m \\ &\quad + \frac{(R+S)}{I_e} T_e + \frac{S}{I_g} T_g - \left(\frac{(R+S)^2}{R I_e K} + \frac{S^2}{R I_g K} \right) C \end{aligned} \quad (11)$$

$$\begin{aligned} \left(\frac{R^2 K I_v}{(R+S) I_v} + \frac{S^2 I_v}{(R+S) I_g} + (R+S) \right) \dot{\omega}_e &= \left(\frac{R^2 K}{(R+S) I_v} \right) \\ &\quad + \frac{S^2}{(R+S) I_g} T_e + \frac{K R}{I_v} T_m - \frac{S}{I_g} T_g - \frac{R}{I_v} C \end{aligned} \quad (12)$$

where

$$I_v = \frac{R_{tire}^2}{K} m + I_m K + I_r K$$

$$I_g = I_g + I_s$$

$$I_e = I_e + I_c$$

$$C = T_{fb} + mgf_r R_{tire} + 0.5\rho A C_d \left(\frac{\omega_r}{K} \right)^2 R_{tire}^3$$

In the derivation above, we assume perfect gear mechanical efficiency (no loss) to simplify the derivation. This idealized assumption again might results in a more optimistic fuel economy prediction.

The vehicle dynamic components linked by the planetary gear are now presented by a two degree of freedom system. Note any two speeds are known, the one speed left will be pre-determined, and can be calculated from Eq.(1). Here we take engine speed and ring gear speed, which is directly related to the vehicle speed, as two states.

In the literature, some of the research work investigates the power split configuration with a sun gear brake [8, 15]. Since the sun gear speed is specified (zero), if a clutch installed to enable the lock-up of the sun gear, the overall vehicle system will only have one degree of freedom. The differential equation will be simplified to

$$(I_v + K I_e \left(\frac{R}{R+S} \right)^2) \dot{\omega}_r = K T_m + K \frac{R}{R+S} T_e - C \quad (13)$$

In this case, the engine speed can be calculated from Eq.(1) with generator speed set at zero. Because no power flows through the generator, 100% of the engine power is transferred to the ring gear. Motor can still be used as a power assist element. The vehicle is turned into a parallel configuration as a special case. In addition, since the speed constraint Eq.(1) becomes

$$\omega_r R = \omega_c (R + S) \quad (14)$$

The planetary gear set only has one fix gear ratio between the engine and the ring gear. This implies that the parallel case can only exist in a certain vehicle speed range due to engine operation constraint. An apparent application is when the vehicle is cruising on the highway. Instead of transferring the engine power through generator to motor, at lower efficiency, directly applying the engine power to the final shafts by locking the sun gear seems a better choice. However, there is no evidence that THS implements such a design.

B. The electrical path

In the electrical path, an inverter is applied to draw/store power from the battery. The battery state of charge (SOC), is the 3rd state of the vehicle system. It relates the battery capacity and the current through

$$SOC = -\frac{I_{batt}}{C_{batt}} \quad (15)$$

where I_{batt} is the battery current and C_{batt} is the battery capacity. An internal resistance model is used, from which the battery power output is

$$P_{batt} = V_{oc} I_{batt} - I_{batt}^2 R_{batt} \quad (16)$$

where V_{oc} is the open circuit voltage and R_{batt} is the battery resistance, both of which are functions of SOC. Note here when P_{batt} and I_{batt} are both positive, the battery is discharged. When they are negative, the battery is charged.

Eq.(16) shows the relationship between battery current and power. However, in the vehicle simulation, we specify the motor and generator power instead of battery current, and the battery power is calculated from

$$P_{batt} = T_m \omega_r \eta_m^{-k} - T_g \omega_g \eta_g^k \quad (17)$$

where η_g and η_m are the efficiency of the generator and the motor respectively. $k=1$ when the battery is discharged and $k=-1$ when the battery is charged. The signs for the motor and the generator terms are different because of the sign convention used in Fig. 3. Specifically, when the velocity and torque of the generator are of the same signs, it is generating energy. When the velocity and torque of the motor are of the same signs, however, it is consuming energy. Based on Eqs. (15)-(17), we have

$$\dot{SOC} = -\frac{V_{oc} - \sqrt{V_{oc}^2 - 4(T_m \omega_r \eta_m^{-k} - T_g \omega_g \eta_g^k)R_{batt}}}{C_{batt}} \quad (18)$$

which is the governing equation of the battery dynamics.

III. CONTROL PROBLEM FORMULATION

Overall, equations (11), (12), and (18) present the governing equations for the three states of THS. The ring gear speed, which directly relates to the vehicle forward speed, the engine speed, and the SOC of the battery are the three states. Torques from the engine, the motor, and the generator are the three inputs. The aerodynamic drag and resistance force of the vehicle give the disturbance of the system. Here since we are ignoring gravity force and we are interested in matching the Prius performance under wide open throttle (WOT) and driving cycles—for which cases it is a common practice to assume flat roads. A multiple inputs multiple outputs (MIMO) control problem is formulated as shown in figure 4.

In Figure 4, Plant $P(s)$ contains the dynamic model we just derived. Actuator $E(s)$, $G(s)$, and $M(s)$ present the relationship between the control signals and the generated torque signals. Compared to the engine dynamic $E(s)$, the generator $G(s)$ and motor $M(s)$ have much faster response. Within their working boundaries, it is reasonable to ignore the dynamics involved in the $G(s)$ and $M(s)$ and represent them by nonlinear algebraic look-up tables. In addition, it is obvious that Eqs. (11) and (12) present a linear relations between the speeds and input torques. If we ignore the temperature effect on the battery, the open circuit voltage can be linearized around SOC. Furthermore, it is possible to linearize the actuator behaviors, or define virtual inputs so

that the actuator mapping can be inverted. The vehicle system is then linear and can be solved by linear feedback control techniques. This linear control design and analysis will be shown in a future work.

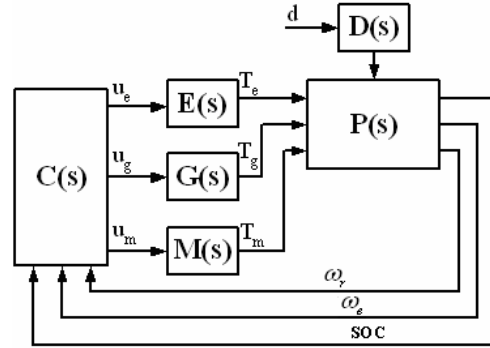


Fig. 4. Close loop of the THS control system.

IV. CONTROL STRATEGY

Even though a linear control approach is possible, as discussed in the previous section, the control algorithms used in many HEV prototype vehicles are rule-based. This is because of the multiple-input and multiple-objective nature of the control problem. It is intuitive that since the engine is the predominant power source—and if we can operate the engine at an efficient manner, the overall vehicle efficiency will be reasonable. This simple idea is an easy way to provide a near-optimal solution quickly, even though there is no guarantee of its closeness to optimality. For engineers pressed for time, the rule-based design strategy is a safe approach.

Hermance [16] presented the basic idea of the rule-based control logic of the THS system. Similar description can be also found in [17]. In the following, a rule-based control strategy is developed following these references to approximate the control law used in the THS.

As shown in the Figure 5, the driving force can be provided by motor and/or engine. When the power demand is low and the battery SOC is sufficiently high, the motor works individually to drive the vehicle. As the vehicle speed increases, power demand increases, or the battery SOC becomes too low, the engine will be started to supply the power. The generator cooperates with the motor to help start the engine. Within the engine operating range, its engine power will be split through the planetary gear system. Part of the power goes to the vehicle driving wheel through the ring gear. The rest drives the generator to charge the battery and/or directly supply the motor power. In other words, although the engine fully supplies the power at this stage, the power is split and executed through two paths, the ring gear to the final wheel and the generator to the motor. As the power demand keeps increasing, the engine might be stretched to operate outside of its efficient range. For those cases, the motor can provide assistant power so that the engine efficiency remains high (as long as the battery is able

to supply power).

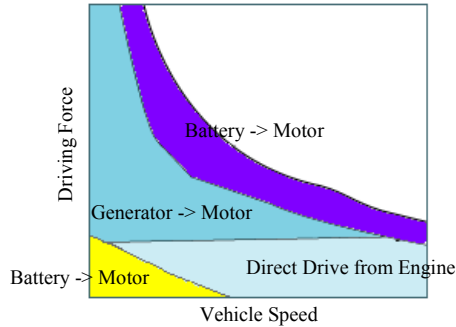


Fig. 5. Power distribution of the Toyota Hybrid System.

When the vehicle decelerates, the regenerative control system commands the motor to operate as a generator to recharge the battery. The friction brake is used whenever the requested braking power exceeds the capability of the motor or the battery. The engine and other components in the THS are set to free-rolling. To simplify the system, the effect of engine brake is ignored. Table I summarizes the basic ideas discussed above.

TABLE I
RULE-BASED POWER TRAIN CONTROL STRATEGY

Conditions	Engine	Motor	Generator
Pd<0 (braking)	0	Min(Pd,Pmax)	0
Pd<Pev w/o charging	0	Pd	0
Pev<Pd<Pemax Or w/ charging	Pd(+Pch)	Pg(-Pch)	Pe-Pr
Pd>Pemax	Pemax	Pg+Pbatt	Pe-Pr

Note the power transfer efficiency is not shown in this table.

Pd = driver demand power, Pmax = motor regenerative maximum power, Pev = electric vehicle boundary power, Pch = battery charging demand power, Pg = generator generated power, Pr = power transferred from engine to the ring gear, Pe = engine output power, Pemax = maximum engine output power, Pbatt = battery output power.

Fig. 6 shows the power split block of the Simulink model for the THS. The rule-based power split control command is given in the *power management control* block. The charging power if necessary is calculated in the *battery charge demand* block. Based on the engine power demand, the engine controller calculates the optimal engine operating point and computes the corresponding engine speed. A *target generator speed* unit then calculates the generator command speed according to the optimal engine speed and the ring gear speed, which is proportional to the vehicle speed. The *generator controller* then manipulates generator torque to achieve the generator speed. In the meantime, the *motor controller* receives a torque command from the *power management control*. The motor power is supplied either through the engine generator path or the battery directly.

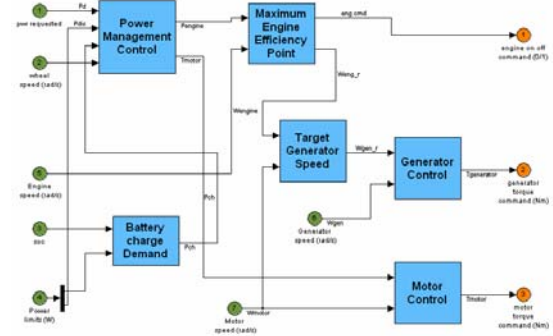


Fig. 6. Power split controller in Simulink.

V. SIMULATION AND DISCUSSION

Fig. 7 shows the top level of the Simulink model for the THS system. A *Driver* model takes reference speed command from the *Driving Cycle* data file, compares it with the simulation speed of the vehicle and gives the driving command. The *Hybrid Controller* block follows the driver command to decide the power split and driving commands. Those command inputs then go to the power source components, *Engine*, *Generator*, and *Electric Motor*, which produce the actual input signals to the plant, *Planetary Gear Set & Vehicle* and *Battery*. Speeds responses are captured and feed back to the control system.

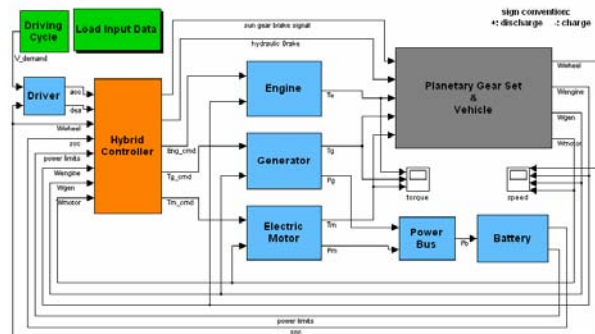


Fig. 7. THS Power train Simulink model.

All the vehicle parameters, engine maps and efficiency look-up tables are obtained from ADVISOR 2002 and [11].

In Fig. 8, the vehicle response under a launching profile, as part of the US06 driving cycle, is presented. Part (a) shows the power from the engine, motor and generator. Note the initial power is supplied solely by the motor and then the engine starts up to drive the vehicle and charge the battery. Part (b) shows the component speeds. The results agree with the experimental results reported in [2] qualitatively.

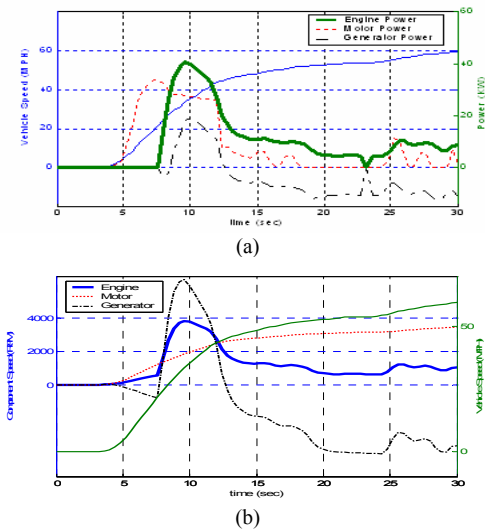


Fig. 8. Vehicle acceleration simulation results [US06].

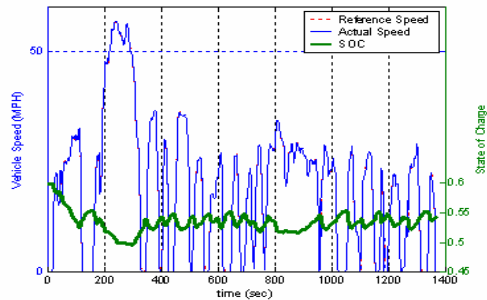


Fig. 9. Vehicle operating simulation results [EPA urban cycle].

TABLE II

FUEL CONSUMPTION COMPARISON

Fuel Consumption (mpg)	2000 Prius	2003 Prius	ADVISOR	Our Simulation
City	43	52	48	57
Highway	41	45	65	54

Note 2000 model is in Japan only.

In Fig. 9, the vehicle speed and battery SOC response under the EPA city cycle are presented. The actual vehicle speed follows the specified speed closely and the battery SOC is kept within a small range—similar to the reported Prius behavior in [11]. The fuel economy results under the EPA cycles are shown in Table II. It can be seen that our model overestimates the fuel economy for both cycles. As stated before, our model ignores friction losses, vehicle auxiliary system load, and secondary inertias. In addition, the simplified engine model omits the throttle control and transient engine operations. A better engine model will be developed as part of our future study to capture the engine behavior more accurately. In addition, we speculate that there maybe practical issues (NVH, drivability, component reliability etc.) that necessitate control patches which negatively impact fuel economy. Judging from the fact the MY2003 Prius, a larger vehicle, achieves better fuel economy, we think the results predicted by our simulation model is very reasonable, compared with the ADVISOR.

VI. CONCLUSION

A dynamic model of the Toyota Prius hybrid system, THS, was developed in this paper. A rule-based controller was implemented to control the overall behavior of the vehicle in a Matlab/Simulink model. Simulation results confirms that the vehicle mimics the behavior of the THS operation reasonable well. This dynamic model is currently used for control and system analysis. We are also exploring configuration, component design and control methods to further improve the vehicle performance.

ACKNOWLEDGEMENTS

This work is partially supported by Automotive Research Center of the University of Michigan, a Center of Excellence sponsored by the U.S. Army TARDEC under the contract DAAE07-98-C-R-L008.

REFERENCES

- [1] Ogawa, H., Matsuki, M., and Eguchi, T., "Development of a Power Train for the Hybrid Automobile – The Civic Hybrid", SAE Paper 2003-01-0083.
- [2] Duoba, M., Ng, H., and Larsen, R., "Characterization and Comparison of Two Hybrid Electric Vehicles (HEVs) – Honda Insight and Toyota Prius", SAE Paper 2001-01-1335.
- [3] Sciarretta, A., Back, M., and Guzzella, L., "Optimal Control of Parallel Hybrid Electric Vehicles", IEEE Transactions on Control System Technology, Vol. 12, No. 3, May 2004.
- [4] Lin, C. C., Peng, H., Grizzle, J. W., Liu, J., and Busdiecker, M., "Control System Development for an Advanced-Technology Medium-Duty Hybrid Electric Truck", SAE Paper 2003-01-3369.
- [5] Waltermann, P., "Modeling and Control of the Longitudinal and Lateral Dynamics of a Series Hybrid Vehicle", Proceedings of the 1996 IEEE International Conference on Control Applications, Dearborn, MI, Sep. 15-18, 1996.
- [6] Jalil, N., Kheir, N. A., and Salman, M., "A Rule-Based Energy Management Strategy for a Series Hybrid Vehicle", Proceedings of the American Control Conference, Albuquerque, New Mexico, Jun. 1997.
- [7] Brahma, A., Guezennec, Y., and Rizzoni, G., "Optimal Energy Management in Series Hybrid Electric Vehicles", Proceedings of the American Control Conference, Chicago, Illinois, Jun. 2000.
- [8] Zhang, H., Zhu, Y., Tian, G., Chen, Q., and Chen, Y., "Optimal Energy Management Strategy for Hybrid Electric Vehicles", SAE Paper 2004-01-0576.
- [9] Duoba, M., Ng, H., and Larsen, R., "In-Situ Mapping and Analysis of the Toyota Prius HEV Engine", SAE Paper 2000-01-3096.
- [10] Ng, H., Anderson, J., Duoba, M., and Larsen, R., "Engine Start Characteristics of Two Hybrid Electric Vehicles (HEVs) – Honda Insight and Toyota Prius", SAE Paper 2001-01-2492.
- [11] Rousseau, A., Sharer, P., and Pasquier, M., "Validation Process of a HEV System Analysis Model: PSAT", SAE Paper 2001-01-0953.
- [12] Wang, W., "Revisions on the Model of Toyota Prius in ADVISOR 3.1", SAE Paper 2002-01-0993.
- [13] Rizoulis, D., Burl, J., and Beard, J., "Control Strategies for a Series-Parallel Hybrid Electric Vehicle", SAE Paper 2001-01-1354.
- [14] Muta, K., Yamazaki, M., and Tokieda, J., "Development of New-Generation Hybrid System THS II – Drastic Improvement of Power Performance and Fuel Economy", SAE Paper 2004-01-0064.
- [15] Haapala, K., Thul, A., Andrasko, S., Muehlfield, C., Bloss, B., Nesbitt, R., and Beard, J. E., "Design and Development of the 2001 Michigan Tech FutureTruck, a Power-Split Hybrid Electric Vehicle", SAE Paper 2002-01-1212.
- [16] Hermance, D., "Toyota Hybrid System", 1999 SAE TOPTEC Conference, Albany, NY, May 1999.
- [17] <http://www.toyota.co.jp/en/tech/environment/th2/system.html>.